Development 127, 851-860 (2000)
Printed in Great Britain © The Company of Biologists Limited 2000
DEV8667

Analysis of *Drosophila* photoreceptor axon guidance in eye-specific mosaics

Timothy P. Newsome, Bengt Åsling* and Barry J. Dickson†

Research Institute of Molecular Pathology, Dr Bohr-Gasse 7, A-1030 Vienna, Austria
*Present address: AstraZeneca Bioinformatics, P.O. Box 34, S-221 00 Lund, Sweden
†Author for correspondence (e-mail: dickson@nt.imp.univie.ac.at)

Accepted 29 November 1999; published on WWW 26 January 2000

SUMMARY

During development of the adult *Drosophila* visual system, axons of the eight photoreceptors in each ommatidium fasciculate together and project as a single bundle towards the optic lobes of the brain. Within the brain, individual photoreceptor axons from each bundle then seek specific targets in distinct layers of the optic lobes. The axons of photoreceptors R1-R6 terminate in the lamina, while R7 and R8 axons pass through the lamina to terminate in separate layers of the medulla. To identify genes required for photoreceptor axon guidance, including those with essential functions during early development, we have devised a strategy for the simple and efficient generation of genetic mosaics in which mutant photoreceptor axons innervate a predominantly wild-type brain. In a large-scale saturation mutagenesis performed using this system, we recovered new alleles of the gene encoding the receptor tyrosine phosphatase PTP69D. PTP69D has previously been shown to function in the correct targeting of motor axons in the embryo and R1-R6 axons in the visual system. Here, we show that PTP69D is also required for correct targeting of R7 axons. Whereas mutant R1-R6 axons occasionally extend beyond their normal targets in the lamina, mutant R7 axons often fail to reach their targets in the medulla, stopping instead at the same level as the R8 axon. These targeting errors are difficult to reconcile with models in which PTP69D plays an instructive role in photoreceptor axon targeting, as previously proposed. Rather, we suggest that PTP69D plays a permissive role, perhaps reducing the adhesion of R1-R6 and R7 growth cones to the pioneer R8 axon so that they can respond independently to their specific targeting cues.

Key words: Axon guidance, Target selection, Visual system, Genetic mosaic, Receptor tyrosine phosphatase, Fasciculation

INTRODUCTION

One of the most remarkable events during animal development is the generation of the intricate patterns of neuronal connectivity that characterise the mature nervous system. With astounding precision, differentiating neurons send out axons that, lead by their growth cones, reliably trace often long and convoluted pathways to find their appropriate synaptic targets. In recent years, studies in both vertebrate and invertebrate systems have revealed several highly conserved families of extracellular guidance molecules, their corresponding receptors, and candidate downstream signalling components (Tessier-Lavigne and Goodman, 1996). Many of the genes essential for axon pathfinding were first identified in genetic screens for aberrant patterns of neuronal connectivity in *C. elegans* or *Drosophila* (Tear, 1999). Screens for axon guidance defects in *Drosophila* have generally relied on the histological examination of axon projections in homozygous mutant animals (Seeger et al., 1993; Kolodziej et al., 1995; Martin et al., 1995; Hummel et al., 1999). Mutations in many genes encoding key axon guidance molecules may not however produce informative phenotypes in homozygous mutant animals. Many functions required for axon guidance in the embryo might be provided redundantly by both the maternal and zygotic genomes, while the analysis of later developmental stages is fraught with the difficulty that many mutations might result in pleiotropic and often obscuring phenotypes, such as early lethality. This latter difficulty is particularly acute in the case of the developing adult visual system, which otherwise represents an excellent model system to investigate some of the fundamental strategies involved in axon guidance, including topographic map formation, target selection, and selective fasciculation and defasciculation.

The *Drosophila* compound eye consists of some 750 ommatidia, each composed of 8 photoreceptor cells and an assortment of non-neuronal accessory cells (for reviews, see Meinertzhagen and Hanson, 1993; Wolff et al., 1997). The photoreceptors can be divided into three classes based on their spectral sensitivity and neuronal connectivity: the outer photoreceptors, R1-R6, and two inner photoreceptors, R7 and R8. Successive columns of photoreceptor clusters are laid down in the eye disc as a wave of differentiation sweeps across the disc from posterior to anterior during the late larval and early pupal stages. The eight photoreceptor axons from each ommatidial cluster fasciculate together, forming an ommatidial bundle that pierces the basement membrane in the eye disc, then extends to the posterior edge of the disc and through the optic stalk to reach the brain. Ommatidial fascicles spread out retinotopically on the lateral surface of the brain before turning medially to penetrate the developing optic lobes. The order in

which photoreceptor axons enter the optic lobe is believed to correspond to the order in which the photoreceptors differentiate in the eye disc: first R8, then R1-R6, and finally R7 (Tomlinson and Ready, 1987; Meinertzhagen and Hanson, 1993; Wolff et al., 1997). The pioneer R8 axon passes through the first optic ganglion, the lamina, to terminate in a superficial layer of the second ganglion, the medulla. R1-R6 axons follow the R8 axon only as far as a glial cell layer near the base of the lamina, while the R7 axon extends through the lamina and beyond the R8 terminus to reach targets in a deeper layer of the medulla.

Intensive research on pattern formation in the eye disc has provided a detailed account of the mechanisms of photoreceptor cell fate specification (for review, see Freeman, 1997). By comparison, relatively little is known of the mechanisms by which photoreceptor axons locate their targets in the optic lobes. Standard genetic screens of homozygous mutant larvae (Martin et al., 1995; Garrity et al., 1996) or adults (Boschert et al., 1990) have defined several genes involved in photoreceptor axon guidance, two of which have now been characterised molecularly. These genes encode an SH3-SH2 adaptor protein, Dock (Garrity et al., 1996), and an Ig superfamily member, IrreC (Ramos et al., 1993). Additionally, examination of photoreceptor axon projections in mutants lacking the p21-activated serine/threonine kinase (Pak) or the receptor tyrosine phosphatase PTP69D has revealed important roles for these proteins during photoreceptor axon pathfinding (Garrity et al., 1999; Hing et al., 1999). Genes such as *Pak* and *Ptp69D*, which also perform important functions during embryonic development, clearly illustrate the need to be able to identify genes required for photoreceptor axon guidance irrespective of any additional functions they may perform during early development. This can be achieved by screening for connectivity defects in genetic mosaics.

Here we describe a strategy that has enabled us to efficiently screen for mutations disrupting the projection patterns of adult photoreceptor axons in genetic mosaics. Using the FLP/FRT system in a tissue-specific manner, we were able to routinely generate mosaic animals in which almost the entire retina was homozygous for a newly induced mutation, while the rest of the animal, including the optic lobes, was composed largely of heterozygous tissue. We have used this strategy in a large-scale mutagenesis screen for mosaic larvae with visual system connectivity defects. In this screen we recovered 3 new alleles of *Ptp69D*, demonstrating the effectiveness of this approach in identifying genes required for photoreceptor axon pathfinding.

PTP69D was first shown to function during motor axon targeting in the embryo (Desai et al., 1996). In this system PTP69D is thought to play a permissive role in axon targeting, allowing specific axons to defasciculate from common motor pathways in order to seek their individual target muscles (Desai et al., 1996, 1997). In the visual system, PTP69D is required for the correct targeting of R1-R6 axons to the lamina (Garrity et al., 1999). On the basis of this targeting defect it was suggested that PTP69D may rather act instructively in the visual system, mediating a specific 'stop' signal for R1-R6 axons in the lamina (Garrity et al., 1999; Kunes, 1999). Our mosaic strategy has now made it possible to also examine the projections of R7 axons in *Ptp69D* mutants. Here we show that R7 axons are also mistargeted in *Ptp69D* mutants, but whereas mistargeted R1-R6 axons overshoot their normal targets, mistargeted R7 axons stop short of their targets. These observations are not readily explained by models in which PTP69D mediates a specific targeting decision. Both types of errors might however result from increased adhesion of R1-R6 or R7 growth cones to the pioneer R8 axon. We therefore suggest that PTP69D may also function permissively in the targeting of photoreceptor axons in the adult visual system. For both motor axons and photoreceptor axons, PTP69D activation may be one of the cues that triggers the transition from fasciculative to independent pathfinding.

MATERIALS AND METHODS

Genetic stocks

FRT chromosomes are those generated by Xu and Rubin (1993). The TM6B,*Tb*,y^+ chromosome was generated by mobilising a *P*[y^+] insertion originally located on a CyO chromosome provided by Konrad Basler (University of Zurich). The *eyFLP2* insertion was recombined onto a *y w glass-lacZ* chromosome provided by Larry Zipursky (UCLA). The three *Ptp69D* alleles we isolated all failed to complement both the $Ptp69D^1$ and $Ptp69D^{8ex25}$ alleles. All other stocks generated or used in this study are listed in Table 1 or in FlyBase (http://flybase.bio.indiana.edu).

Transgenic constructs

eyFLP

A 258 bp eye-specific enhancer fragment from the *ey* gene (nucleotides 2549-2806, GenBank accession no. AJ131630; Hauck et al., 1999) was amplified from genomic DNA by PCR. This fragment includes the 212 bp element reported by Hauck et al. (1999) to be necessary and sufficient for eye-specific expression. The PCR primers provided flanking *Bam*HI and *Bgl*II sites. Four copies of the PCR product were cloned in successive steps as *Bam*HI-*Bgl*II fragments into a vector containing the non-inducible *hsp70* promoter (nucleotides 479-926, GenBank accession no. V00213), which had also been amplified from genomic DNA. This enhancer-promoter fragment was then inserted upstream of a *FLP* cDNA in a pCarnegie20-based vector (provided by K. Basler) for germline transformation. Most of the experiments reported here were performed using an *eyFLP* insertion on the X chromosome (*eyFLP2*), which had been recombined into a y^{d2} w^{1118} background. The *eyFLP5* insertion on the second chromosome was used to generate clones on the X.

GMR-Ptp69D

The *Ptp69D* cDNA was constructed from the full length EST clone LD09678 (Berkeley *Drosophila* Genome Project), modified by standard PCR-based procedures to replace the 5′ sequences encoding the PTP69D signal sequence with a fragment encoding the wingless signal sequence followed by 3 copies of the hemagglutinin epitope tag (provided by K. Basler). This modified *Ptp69D* cDNA was then inserted into a pCaSpeR-based transformation vector containing 5 tandem copies of the glass binding site from the *Rh1* promoter and the uninducible *hsp70* promoter. This vector is essentially identical to the pGMR vector described by Hay et al. (1994). The rescue experiment was performed using a *GMR-Ptp69D* insertion on the second chromosome.

Rh1-τlacZ and *Rh4-τlacZ*

The *Rh1* and *Rh4* promoters were cloned as *Bgl*II-*Asp*718 and *Not*I-*Asp*718 fragments respectively from the plasmids pDM55 and pRh4-6 provided by Gerry Rubin (Mismer and Rubin, 1987; Fortini and Rubin, 1990), together with an *Asp*718-*Xba*I *τlacZ* fragment from a

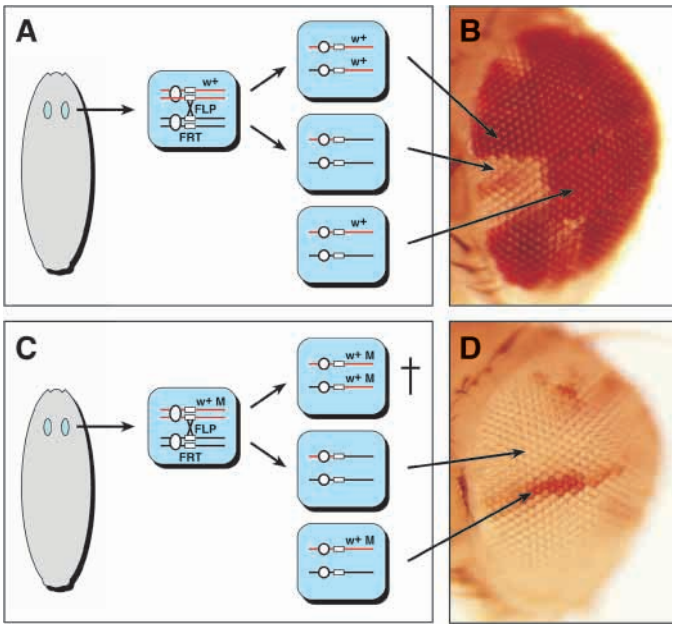

Fig. 1. Generation of genetic mosaics with the *eyFLP* system. (A) FLP recombinase is expressed in the cells of the developing eye (blue). A w^+ marker distal to an *FRT* insertion on one chromosome arm allows mosaicism to be detected in a w^- background. Site-specific mitotic recombination at the *FRT* site produces daughter cells either homozygous for or lacking the w^+ marker. (B) Adult eyes of *y w eyFLP2*; *P*[w^+] *FRT80B*/*FRT80B* flies are a mosaic of pigmented (heterozygous or homozygous for the w^+ marker) and unpigmented (lacking the marker) tissue. (C) In an extension of this system, *Minute* or cell lethal mutations (indicated by M) can be used to eliminate clones derived from one of the homozygous cells following recombination. (D) Adult eyes of *y w eyFLP2*; *M(3)RpS17*^{4} *P*[w^+] *FRT80B*/*FRT80B* flies consist almost entirely of cells homozygous for the unmarked chromosome arm.

clone provided by Chris Callahan (Callahan and Thomas, 1994), into a pCaSpeR-based transformation vector. *Rh1-τlacZ* and *Rh4-τlacZ* insertions on the second chromosome were used.

Mutagenesis

To generate mutations that would enhance the size of *eyFLP*-induced clones, *y w eyFLP1*; *FRT P*[w^+] males were starved for 12 hours, then fed 25 mM ethanemethanesulfonate (EMS; Fluka) in 1% sucrose for 24 hours. After a 24-hour recovery period, the mutagenised males were mated to the corresponding *y w eyFLP1*; *FRT* virgin females. The progeny of these crosses were screened for animals with smooth eyes almost entirely lacking w^+ pigment. This screen was performed for each of the four major autosomal arms, and in each case such mutations were recovered at a frequency of approximately 1:500 progeny. These mutations were retested and reisogenized, and a selected mutation for each arm was then crossed into an *eyFLP2* background to establish the stocks listed in Table 1. For chromosome arm 3L, the stocks carrying the *Minute* mutation *M(3)RpS17*^{4} were healthy and fertile, and so for 3L this *Minute* was generally used rather than the cell lethal *cl3L5*.

Mutations disrupting photoreceptor axon projections were isolated according to the scheme shown in Fig. 3. Male flies were treated with EMS as described above. Approximately 30% of the F_1 progeny showed an abnormal external eye morphology and were discarded. Single smooth-eyed F_1 males were then crossed to the appropriate *Minute* or *cl* females, and mosaic F_2 larvae were identified by selecting against the y^+ or *Tb* markers on the balancer chromosomes. Eye-brain complexes from 2-3 late third instar larvae were dissected, fixed and stained for β-galactosidase activity. Photoreceptor axon projections were examined under a Leica stereo dissecting microscope at 100× magnification. From the lines selected in this primary screen, those in which the F_2 mosaic adults had rough eyes were discarded and the remaining F_2 lines retested 'blind' by crossing the mosaic males back to the corresponding *Minute* or *cl* stock and dispersing these crosses at random amongst the primary lines. Those that retested positive were then isogenised and the mutant phenotype confirmed using mAb24B10.

Sequence analysis of *Ptp69D* alleles

Genomic DNA was prepared from adult flies heterozygous for a *Ptp69D* allele and the TM6B balancer chromosome. The *Ptp69D* gene was amplified in four separate polymerase chain reactions that together included the entire *Ptp69D* coding region. PCR products were completely sequenced in both directions on an ABI 377 and polymorphisms detected by the occurrence of overlapping signals in the chromatograph. For each of the three alleles, one and only one allele-specific polymorphism was detected: D1515: CAG(Q931)→TAG(stop); D1689: TGG(W54)→TAG(stop); and H24: GGA(G1105)→AGA(R).

Histology and immunohistochemistry

Larval eye-brain complexes were dissected and stained for β-galactosidase activity as described in Mismer and Rubin (1987). Whole-mount immunofluorescent stainings were performed as

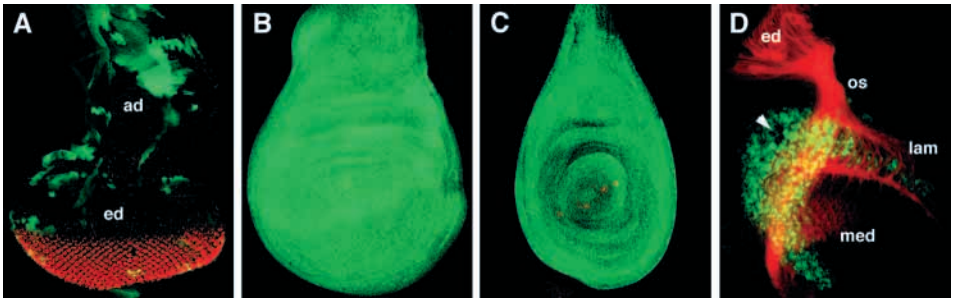

Fig. 2. Tissue-specific mosaicism induced by *eyFLP*. (A-C) Imaginal discs dissected from third instar larvae of the genotype *y w eyFLP2*; *FRT82B P*[w^+,*arm-lacZ*] *M(3)RpS3*^{2}/*FRT82B*, and stained with antibodies against β-galactosidase (green) and the neuronal antigen Elav (red). (A) The eye disc (ed) consists almost entirely of cells homozygous for the unmarked chromosome arm. A high degree of mosaicism is also observed in the associated antennal disc (ad). Wing (B) and leg (C) discs do not show any mosaicism. (D) An eye-brain complex from a larva of the genotype *y w eyFLP2*; *P*[w^+,*S14-lacZ*] *M(3)RpS17*^{4} *FRT80B*/*FRT80B* stained with mAb24B10 to visualize photoreceptor axons (red) and anti-β-galactosidase antibodies to visualize lamina precursor cells (green). Photoreceptor axons project from the eye disc (ed), through the optic stalk (os) and into the optic lobe. R1-R6 axons terminate in the lamina (lam), while R7 and R8 axons terminate in the medulla (med). At this early stage, few if any R7 axons have reached the medulla. Cells of the developing lamina are generally heterozygous and only small and infrequent homozygous patches can be detected (arrowhead).

Table 1. Stocks for the generation of eye-specific mosaics

eyFLP insertion	Mosaic arm	Genotype
X		*y w eyFLP1*
X		*y w eyFLP2*
2		*y w*; *eyFLP*5
3		*y w*; *eyFLP*6
X		*y w eyFLP2 glass-lacZ*
2	X	*FRT19A*; *eyFLP*5
2	X	*y w FRT19A*; *eyFLP*5
X	2L	*y w eyFLP2 glass-lacZ*; *M(2)24F*^{1} *w*$^+$ *FRT40A*/CyO, *y*$^+$
X	2L	*y w eyFLP2 glass-lacZ*; *cl2L3 w*$^+$ *FRT40A*/CyO, *y*$^+$
X	2L	*y w eyFLP2 glass-lacZ*; *FRT40A*
X	2R	*y w eyFLP2 glass-lacZ*; *FRT42D w*$^+$ *M(2)58F*^{1}/CyO, *y*$^+$
X	2R	*y w eyFLP2 glass-lacZ*; *FRT42D w*$^+$ *cl2R11*/CyO, *y*$^+$
X	2R	*y w eyFLP2 glass-lacZ*; *FRT42D*
X	3L	*y w eyFLP2 glass-lacZ*; *M(3)RpS17*^{4} *w*$^+$ *FRT80B*/TM6B, *y*$^+$
X	3L	*y w eyFLP2 glass-lacZ*; *cl3L5 w*$^+$ *FRT80B*/TM6B, *y*$^+$
X	3L	*y w eyFLP2 glass-lacZ*; *FRT80B*
X	3R	*y w eyFLP2 glass-lacZ*; *FRT82B w*$^+$ *M(3)RpS3*^{2}/TM6B, *y*$^+$
X	3R	*y w eyFLP2 glass-lacZ*; *FRT82B w*$^+$ *cl3R3*/TM6B, *y*$^+$
X	3R	*y w eyFLP2 glass-lacZ*; *FRT82B*

cl2L3, *cl2R11*, *cl3L5* and *cl3R3* are the cell lethal mutations induced to eliminate the twin spot. All *FRT* chromosomes are derived from those of Xu and Rubin (1993). Most of these stocks are available from the Bloomington Drosophila Stock Center (http://flystocks.bio.indiana.edu).

described by Kunes et al. (1993), except that samples were fixed in PLP (0.075 M lysine, 4% paraformaldehyde, 0.01 M $NaIO_4$, 0.037 M phosphate buffer, pH 7.4), blocked in PBT (PBS, 0.3% Triton X-100) with 5% goat serum, and mounted in SlowFade Light (Molecular Probes). Primary antibodies were mAb24B10 (1:150, kindly provided by Larry Zipursky), rabbit anti-β-galactosidase (1:2500, Cappel), and mAb9F8A9 against Elav (1:30, generated by Gerry Rubin and obtained from the Developmental Studies Hybridoma Bank, University of Iowa). Secondary antibodies were A488-conjugated goat anti-rabbit (1:200, Molecular Probes) and Cy3-conjugated goat anti-mouse (1:200, Jackson Immunoresearch).

Adult head sections stained with diaminobenzidine (DAB) were prepared as follows. Heads were prefixed in 2% formaldehyde in PBS, washed several times in PBS, incubated overnight in 12% sucrose in PBS at 4°C, and mounted in OCT medium (Tissue-Tek). 10 μm sections were collected on poly-L-lysine coated slides, immediately postfixed in 0.5% formaldehyde for 20 minutes, washed in PBT (3× 5 minutes), blocked for 30 minutes in PBT-BSA (PBT, 1% BSA) and then incubated overnight at 4°C in a 1:150 dilution of mAb24B10 in PBT-BSA. Slides were then washed in PBT and incubated for 30 minutes with HRP-conjugated goat anti-mouse secondary antibody (Jackson Immunoresearch) diluted 1:500 in PBT-BSA. Finally slides were washed in PBT, incubated with DAB (0.3 mg/ml DAB, 0.003% H_2O_2) for 20 minutes, rinsed with PBS and mounted in PBS with 70% glycerol. Immunofluorescent staining of adult head sections was performed as described in Chou et al. (1999). mAb24B10 was used at 1:150 and mAb22C10 (generated by Seymour Benzer and obtained from the Hybridoma Bank) was used at 1:50.

RESULTS

Simple and efficient induction of mitotic clones with *eyFLP*

We used the FLP/FRT system (Golic, 1991; Xu and Rubin, 1993) to generate homozygous mutant clones by site-specific mitotic recombination. To restrict recombination to the developing visual system, we placed the *FLP* cDNA under the transcriptional control of four tandem copies of a 258 bp eye-specific enhancer from the *eyeless* (*ey*) gene and a basal *hsp70* promoter. The *ey* enhancer fragment we used in this *eyFLP* construct does not recapitulate the entire expression pattern of the *ey* gene, but is exclusively expressed in the visual system (Hauck et al., 1999). Expression begins in the 6-23 cell eye-disc primordium in the stage 15 embryo and is maintained until the final cell divisions in the approx. 15000-cell disc of the late third instar larva. A lower level of expression can also be detected in the optic lobes (U. Walldorf, personal communication). We anticipated that this multimerized eye-specific enhancer would provide continuous high levels of FLP activity throughout the entire proliferative phase of eye development, resulting in a high frequency of eye-specific mosaicism (Fig. 1A).

To test this system, we first generated mosaics using an X-chromosomal *eyFLP* insertion and a *white*$^+$ (*w*$^+$) marker located distal to an autosomal *FRT* insertion. Mosaicism was induced with similar efficiency for each of the four major autosomal arms. In all cases, both eyes of every single heterozygous animal were mosaic for the *w*$^+$ marker, typically composed of 20-30% homozygous *w*$^-$ tissue and 70-80% heterozygous or homozygous *w*$^+$ tissue (Fig. 1B). Using an autosomal *eyFLP* insertion we were also able to induce X-chromosomal mosaics with similar efficiency. The degree of mosaicism was remarkably consistent, in contrast to the variable degree of mosaicism generally observed when the FLP recombinase is expressed under heat shock control. The reproducibility of this method presumably derives from the use of a developmentally regulated enhancer to provide constant levels of recombinase activity.

Heterozygous flies with homozygous eyes

To further increase the size of the *w*$^-$ clone, we recombined *Minute* mutations onto the marked *w*$^+$ *FRT* chromosome arms (Fig. 1C). *Minute* mutations prevent the proliferation or survival of homozygous cells, and retard the proliferation of heterozygous cells (Morata and Ripoll, 1975). In such *eyFLP*-induced mosaics, the eye now typically was composed of 90-100% *w*$^-$ tissue (Fig. 1D), depending on the *Minute* mutation used.

The *w*$^+$ marker only allowed examination of *eyFLP*-induced mosaicism in the adult eye. To test for mosaicism in other tissues, we generated clones using a ubiquitous *arm-lacZ* reporter. The marked arm additionally carried a *Minute* mutation. Mosaic larvae were dissected, fixed and stained for β-galactosidase immunoreactivity to distinguish homozygous (unstained) from heterozygous (stained) tissue. As expected, the eye imaginal disc consisted almost entirely of homozygous tissue. Large homozygous patches could also be observed in the associated antennal disc (Fig. 2A). In contrast, other imaginal discs consisted entirely of heterozygous tissue (Fig. 2B,C). Thus, the *eyFLP* transgene drives mitotic recombination exclusively in the eye-antennal imaginal disc.

Analysing mosaicism in the complex three-dimensional structure of the larval CNS proved difficult using the ubiquitous *arm-lacZ* marker. To visualize any clones that might be induced in the optic lobes, we used, instead, a lamina-specific marker, *S14-lacZ* (Mozer and Benzer, 1994). Using this marker, together with a *Minute* mutation, we could detect only small and infrequent homozygous clones in the lamina (Fig. 2D). We have not examined mosaicism in other regions

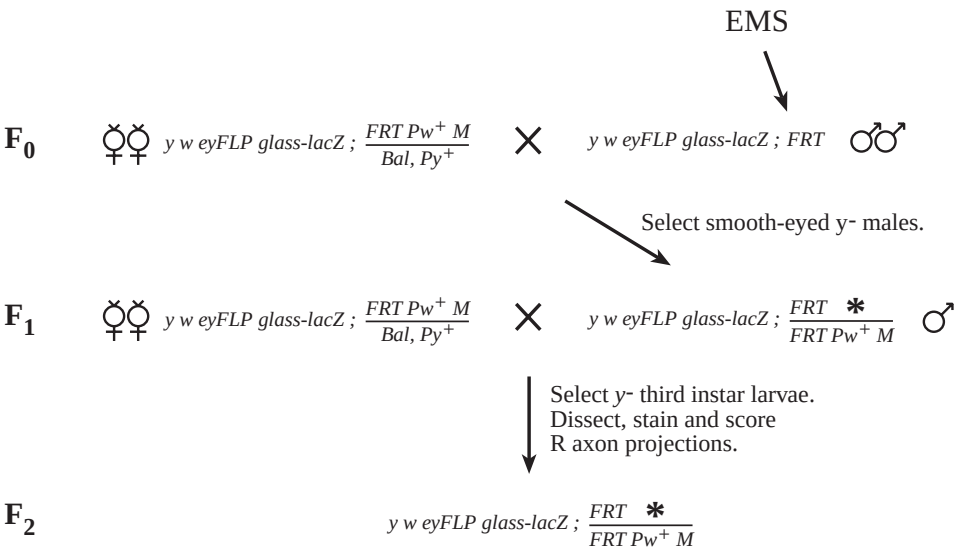

Fig. 3. Genetic screen for the recovery of mutations disrupting adult photoreceptor axon projections. For details, see Results and Materials and Methods. The asterisk indicates a newly induced recessive mutation, made homozygous in the eyes of F_1 and F_2 animals. M indicates either the *Minute* or cell lethal mutation used to eliminate the twin spot. Animals homozygous for *M* die before reaching the third larval instar stage, and so selection against the balancer chromosome ensures that mosaic larvae are dissected in the F_2 generation.

of the CNS, but given the restricted expression of the *ey* enhancer, we anticipate that, as for the other imaginal tissues, these will be predominantly, if not exclusively, heterozygous. Thus, using the *eyFLP* system together with *Minute* mutations, we could routinely generate mosaic animals in which homozygous photoreceptor axons innervate a predominantly heterozygous brain.

Finally, since *Minute* mutations are generally associated with developmental retardation, low viability and reduced fertility, and thus do not lend themselves well to large scale genetic screens, we screened directly for other mutations that would similarly enhance the size of *eyFLP*-induced clones, but not have such deleterious effects on viability and fertility. We mutagenized *FRT* w^+ chomosomes and crossed these flies to the corresponding unmarked *FRT* stocks, in the presence of *eyFLP*, and screened directly for progeny with over 80% w^- tissue in the adult eye. Such mutations, most likely recessive cell lethal mutations (and hence referred to as *cl* mutations), were isolated with high efficiency. We and others (E. Hafen, pers. comm.; J. O'Tousa, pers. comm.) have verified that these *cl* mutations do not disrupt development or function of the visual system when used in conjunction with the *eyFLP* system, and their greater viability and fertility compared to *Minute* mutations has made them indispensable for large scale genetic screens (this report; E. Hafen, pers. comm.; J. Knoblich, pers. comm.). These stocks are listed in Table 1.

Mosaic screen for visual system connectivity mutants

Using the *eyFLP* strategy, together with either *Minute* or *cl* mutations, we have recently completed a large-scale genetic screen of the four major autosomal arms for mutations that disrupt the pathfinding capabilities of photoreceptor axons. A detailed report of the mutants recovered in this screen is in preparation (T. P. N., B. Å., B. J. D., unpublished). Here, we describe the basic strategy of this screen to illustrate the utility of the *eyFLP* system in identifying and analysing mutations disrupting photoreceptor axon guidance in particular, and visual system development and function in general.

The mutagenesis strategy is outlined in Fig. 3. A *glass-lacZ* reporter was used to enable rapid visualization of connectivity patterns by staining for the β-galactosidase activity present in all photoreceptor axons (Moses and Rubin, 1991). Males carrying the *eyFLP* construct, the *glass-lacZ* reporter, and a recently isogenised *FRT* chromosome were treated with ethanemethanesulfonate and crossed en masse to females carrying the corresponding *Minute* or *cl FRT* chromosome. The mosaic F_1 progeny from this cross could potentially have been screened for connectivity defects, were there a reliable non-invasive means of visualizing photoreceptor axons in live adult flies. Since this was not possible, individual mosaic males were then backcrossed to the *Minute* or *cl* strain. The fact that the F_1 flies were themselves mosaic did however allow us to exclude from further analysis all those mutations that resulted in a roughening of the eye surface, a reliable indicator of patterning defects in the retina. From a total of 32,175 F_1 backcrosses, mosaic third instar F_2 larvae were dissected and their eye-brain complexes stained for β-galactosidase activity. Those lines showing abnormal projection patterns in all hemispheres examined were retested 'blind', before being re-isogenised and retested a third time using mAb24B10, which labels all photoreceptors and their axons (Fujita et al., 1982). Adult eyes were then sectioned tangentially and examined to ensure that most ommatidia contained the normal complement and arrangement of photoreceptor cells. At the end of this

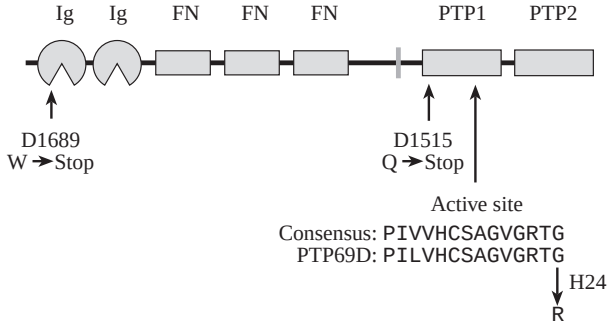

Fig. 4. Mutations in PTP69D. PTP69D consists of two immunoglobulin domains (Ig), three fibronectin type three domains (FN), a single transmembrane region, and two cytoplasmic tyrosine phosphatase domains (PTP1 and PTP2). The three mutations we isolated either truncate the protein before the catalytic domains (D1689 and D1515) or exchange an invariant glycine residue flanking the active site of the PTP1 domain (H24).

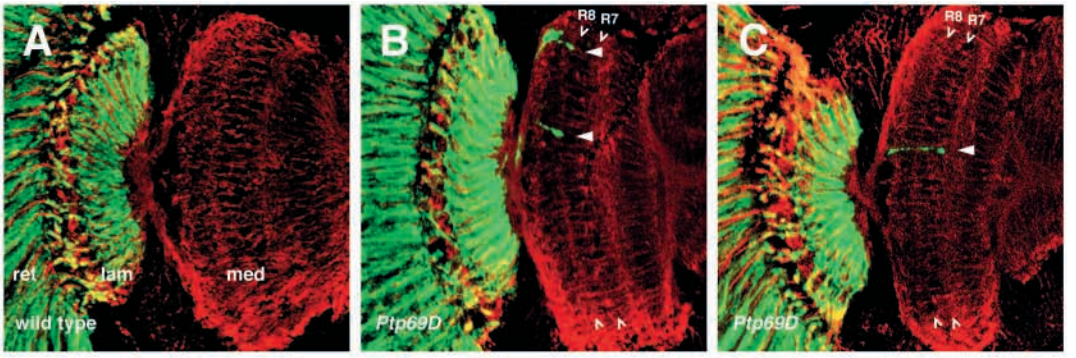

Fig. 5. R1-R6 targeting errors in *Ptp69D* mosaics. Adult head sections of flies carrying the *Rh1-τlacZ* reporter stained with anti-β-galactosidase (green) to visualize the R1-R6 photoreceptors and their axonal projections, and mAb22C10 (red) to visualize all neurons and their processes. (A) In wild-type flies, all R1-R6 axons terminate in the lamina (ret, retina; lam, lamina; med, medulla). (B,C) In *Ptp69D* mosaics, some R1-R6 axons continue through the lamina to terminate in the medulla (arrowheads). The mAb22C10 counterstain reveals the level of R8 and R7 axon termini in the medulla (chevrons). Mistargeted R1-R6 axons terminate at the same level as either R8 (B) or R7 (C) axons.

procedure we retained a total of 210 lines in which the photoreceptor cell fates are correctly specified, but their axons project abnormally into the optic lobes.

Identification of mutations in *Ptp69D*

One of the complementation groups identified in this screen, consisting of the three alleles D1515, D1689 and H24, was mapped by meiotic recombination to position 3-39 on chromosome arm 3L. The gene *Ptp69D* also maps to this region. *Ptp69D* had previously been shown to function in the targeting of motor axons during embryogenesis (Desai et al., 1996), and has since been shown to also function in photoreceptor axon guidance (Garrity et al., 1999). We therefore tested our alleles for complementation with existing *Ptp69D* alleles, and found that they are indeed new alleles of *Ptp69D*.

Ptp69D encodes a receptor tyrosine phosphatase (RPTP). The extracellular domain consists of two immunoglobulin repeats followed by three fibronectin type III repeats. The cytoplasmic domain, like that of most other RPTPs, consists of two tandem tyrosine phosphatase domains. We sequenced the entire *Ptp69D* open reading frame from the three alleles we had isolated and found a single point mutation in each of them: D1689 is predicted to encode a protein truncated in the first Ig domain, D1515 a protein truncated shortly after the transmembrane domain, and H24 a full-length protein in which arginine replaces an invariant glycine residue flanking the active site of the first phosphatase domain (Fig. 4). By genetic criteria, all three alleles are null mutations. We have not observed any dominant phenotypes associated with the truncation of the cytoplasmic domain in the $Ptp69D^{D1515}$ allele, as might be expected if the truncated protein were able to associate with the full-length protein to form either activated or non-functional heterodimers (Weiss and Schlessinger, 1998). The fact that a point mutation in the first phosphatase domain behaves as a genetic null is also consistent with models in which the second domain has little or no catalytic activity on its own, but rather acts as a docking site for signal transduction components such as the cytoskeletal regulator Enabled/Mena (Streuli et al., 1990; Wills et al., 1999).

Multiple targeting errors in *Ptp69D* mosaics

We have analysed in detail the phenotypes associated with the $Ptp69D^{H24}$ allele. The same defects were seen at similar frequencies with both of the other alleles. All analysis was performed on individuals of the genotype: *y w eyFLP2*; $Ptp69D^{H24}$ *FRT80B* / *M(3)RpS17*^{4} *P*[w^{+}] *FRT80B*, carrying additional transgenes as indicated. For simplicity, we refer to such animals as *Ptp69D* mosaics.

Garrity et al. (1999) have previously shown that in homozygous *Ptp69D* mutants, the axons of R1-R6, which normally terminate in the lamina, instead project through the lamina to terminate in the medulla. Using a *Rh1-τlacZ* marker, we observe similar defects in *Ptp69D* mosaic adults (Fig. 5). In a total of 34 hemispheres sectioned, 32 *Rh1-τlacZ*-expressing axons or axon bundles penetrated the medulla. 18 of these terminated at approximately the same level as the R8 axon (Fig. 5B), 14 at the level of the R7 axon (Fig. 5C). Since each section typically contained axons from approximately 20 ommatidia, we estimate that approximately 5% of ommatidial fascicles include one or more mistargeted R1-R6 axons. Using a *ro-τlacZ* marker to label R2-R5 axons in homozygous *Ptp69D* larvae, Garrity et al. (1999) estimated that one or more of these axons projects aberrantly into the medulla in 20-25% of ommatidial bundles. This difference may reflect the different alleles, genetic backgrounds or markers used in these experiments, or a retraction or degeneration of some of the mistargeted R1-R6 axons during the pupal stage.

To further investigate the role of *Ptp69D* in photoreceptor axon targeting, we also examined the projections of R7 and R8 axons. These axons normally pass through the lamina to reach targets in distinct layers of the medulla, R7 axons extending deeper than R8 axons. (Fig. 6A). In adult head sections of *Ptp69D* mosaics stained with mAb24B10 to label all photoreceptor axons, we observed frequent gaps in the array of R7 axon termini in the medulla (Fig. 6B). The array of axon termini at the R8 level was slightly irregular, but appeared uninterrupted. In a total of 11 hemispheres examined, 115 of 246 R7 axons (47%) failed to reach their normal target layer in the medulla. To verify that these defects were not due to a failure to specify the R7 cell fate, we examined tangential sections of *Ptp69D* mosaic eyes and found that R7 was missing in only 1% of ommatidia (10/918). This low frequency of missing R7 cells cannot account for the missing R7 axon termini in the medulla. Since we never observed any grossly misrouted axons in Ptp69D mosaics, we suspected the misrouted R7 axons had followed normal photoreceptor axon pathways, but terminated prior to reaching the deeper layer of the medulla.

To locate these mistargeted R7 axons, we introduced into *Ptp69D* mosaics a transgene carrying a *Rh4-τlacZ* reporter. This axonal marker is expressed in approximately 70% of R7 axons (Fig. 6D). In *Ptp69D* mosaics, we found that many R7 axons terminated prematurely within the medulla at the same level as the R8 axons (Fig. 6E). Three-dimensional reconstructions of these sections confirmed that these axon termini were contained entirely within the section, and do not simply represent axons artificially truncated by the sectioning procedure (Fig. 6F). The large number of labelled R7 axons passing through the lamina unfortunately makes it difficult to determine whether any of them also terminate prematurely within this neuropil. The proportion of R7 axons terminating at the level of R8 axon termini is however sufficient to account for the missing R7 termini deeper in the medulla.

Expression of *Ptp69D* under the eye-specific promoter *GMR* rescues the R1-R6 targeting defect in *Ptp69D* homozygotes (Garrity et al., 1999). We confirmed that a *GMR-Ptp69D* transgene also completely rescues the R7 targeting defect in *Ptp69D* mosaics (Fig. 6C). Thus, the R7 targeting defect, like the R1-R6 targeting defect, is due to the loss of *Ptp69D* function in the eye. Unfortunately, no R7-specific promoter is available to drive *Ptp69D* expression exclusively in R7 cells at the time of axon extension, and so we cannot formally exclude the possibility that the mistargeting of R7 axons in *Ptp69D* mosaics is due to the loss of *Ptp69D* function in retinal cells other than R7. However, the much higher frequency of R7 compared to R1-R6 targeting errors suggests that R7 is not simply mistargeted as an indirect consequence of R1-R6 targeting errors.

In conclusion, both R1-R6 and R7 axons are mistargeted in *Ptp69D* mosaics. As previously reported (Garrity et al., 1999), R1-R6 axons occasionally extend beyond the lamina to terminate in the medulla at the level of either R7 or R8 axon termini. More frequently, R7 axons fail to reach their target layer in the medulla, and often terminate instead at the level of R8 termini. R8 axons, by contrast, appear to be correctly targeted in *Ptp69D* mosaics.

DISCUSSION

eyFLP: a powerful new tool for genetic analysis of the visual system

The *Drosophila* visual system has proved to be an extremely amenable model system for the genetic analysis of many different biological processes (Thomas and Wassarman, 1999). Many important insights into the mechanisms, not only of axon guidance, but also cell cycle control, pattern formation, cell-cell signalling, cell death, and sensory physiology, have come from genetic studies of the *Drosophila* eye. One of the major strengths of the eye as a model system is that it is not essential for the viability or fertility of the organism in the laboratory. One of its major limitations has been that many of the genes required for its development or function are essential. To isolate and analyse mutations in such essential genes, Golic (1991) and Xu and Rubin (1993) adapted the yeast FLP/FRT system for site-specific recombination to the generation of homozygous mutant clones by mitotic recombination in *Drosophila*. While this method has greatly assisted the recovery and analysis of mutations in such essential genes, there are many situations in which the generation of random, negatively labelled clones is of only limited benefit. In particular, it would be impossible to follow the projections of a small group of unlabelled photoreceptor axons into the brain. Furthermore, neuronal connectivity appears to be 'over-

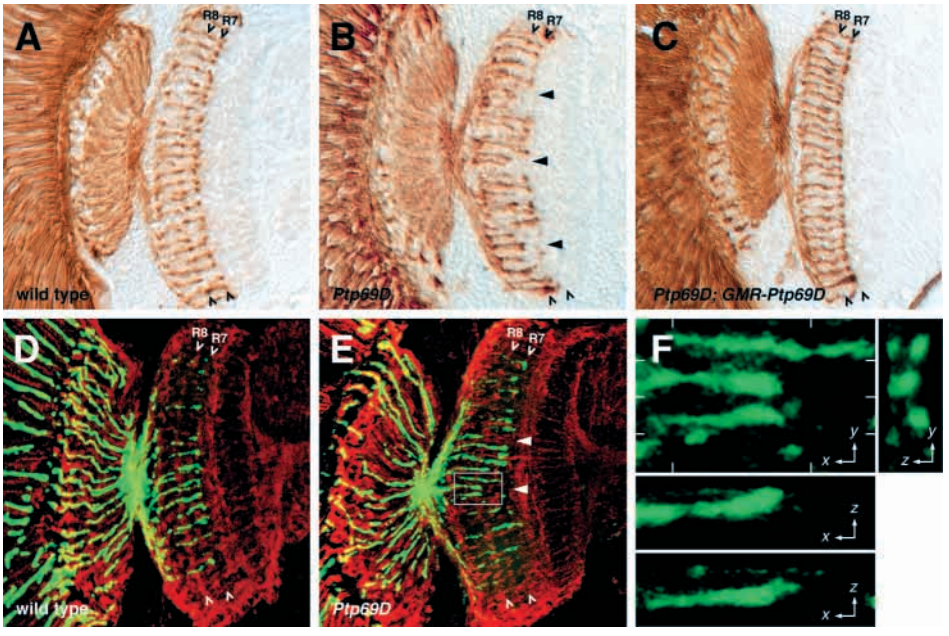

Fig. 6. R7 targeting errors in *Ptp69D* mosaics. (A-C) Adult head sections stained with mAb24B10 to visualize all photoreceptor axons. (A) In wild-type flies, an uninterrupted array of R8 and R7 axon termini can be seen in the medulla (chevrons). (B) In *Ptp69D* mosaics, many R7 axons fail to reach their normal target layer (arrowheads). (C) A *GMR-Ptp69D* transgene rescues the R7 targeting defect in *Ptp69D* mosaics. (D-F) Adult head sections of flies carrying a *Rh4-τlacZ* reporter stained with anti-β-galactosidase (green) to visualize R7 axons and mAb22C10 (red) to visualize all axonal pathways. (D) In wild-type animals, all R7 axons terminate at the same level deep within the medulla. Note that the *Rh4-τlacZ* reporter labels only approximately 70% of the R7 axons. The mAb22C10 counterstain reveals the more superficial layer in which R8 axons terminate. No R7 axons terminate in this layer. (E) In *Ptp69D* mosaics, many R7 axons terminate more superficially, approximately at the level of the R8 axon termini (arrowheads). Chevrons indicate the normal target layers of R8 and R7 axons. (F) A higher magnification of the area boxed in E, showing only the green (anti-β-galactosidase) channel. Two *Rh4-τlacZ*-positive axons terminate in the wrong layer. Z-sections (below and right of the main panel) show that these axons terminate within the section, and have not been truncated during sectioning. White marks in the main panel delimit the regions averaged in the three Z-sections. The two Z-sections below the main panel are delimited by the upper and lower pairs of horizontal marks respectively.

specified' (Goodman, 1996), and in many cases a mutation in a single gene results in only a low frequency of guidance errors. Detecting such infrequent defects would be extremely difficult in random genetic mosaics. The *eyFLP* system overcomes these difficulties by allowing the generation of animals in which virtually the entire retina is homozygous mutant.

The development of this system enabled us to perform a large-scale saturation mutagenesis to identify many of the genes required for photoreceptor axon guidance. Apart from its chief advantage in allowing the recovery of mutations in essential genes, the *eyFLP* system also offers two important features that proved to be of great practical value during this screen. First, by generating homozygous mutant clones in heterozygous animals, it is possible to screen one generation earlier than in a conventional screen of homozygous animals. In many cases this would allow screening in the F_1 generation, but even in our case, screening the F_2 rather than the F_3 progeny saved a considerable amount of labour. This saving could then be invested in screening larger numbers of mutant lines and thus obtaining much greater coverage. Although we could not screen them directly, the fact that the F_1 progeny were also mosaic did at least allow us to eliminate very early in the screening procedure those mutations that produced severe patterning defects in the eye, and were thus unlikely to give rise to informative connectivity defects. Thus, not only could we screen larger numbers of mutant lines than in previous homozygous screens, these lines had already been preselected according to our secondary selection criteria. A second important practical consideration was that the expression of FLP recombinase under developmental rather than heat shock control provided a remarkably consistent degree of mosaicism and also obviated the need to apply a heat shock to each of the many thousands of lines we screened.

This mosaic approach does however have certain limitations. One obvious and unavoidable limitation in any FLP/FRT approach is that one can only assay genes located distal to *FRT* sites, and only those genes for which it is possible to recover homozygous mutant clones. Also, at present it is only possible to generate clones for one chromosome arm at a time, though our preliminary experiments suggest that, once the appropriate stocks are available, it might be possible to simultaneously make at least two arms homozygous. This would allow much greater flexibility in the generation of double mutant combinations. In our screen for connectivity mutants, another important consideration is that large mutant clones are only generated in the retina, not the optic lobe. Our screen was therefore heavily biased towards those genes that act autonomously in the photoreceptors, and we are unlikely to have recovered mutations in genes encoding extracellular guidance cues present in the optic lobe. Other limitations of our screen were imposed by the choice of marker and assay, and both the primary and secondary selection criteria. Future screens might, for example, utilize different markers to address specific guidance decisions (such as retinotopic mapping or the establishment of neuronal superposition), different assays (such as GFP-based or behavioural assays that might allow screening in the F_1 generation), and different selection criteria (for specific errors, and perhaps irrespective of any associated patterning defects in the retina). Also, similar screens could be envisioned to isolate recessive modifiers of the projection defects in certain gain-of-function or possibly even loss-of-function genetic backgrounds.

The *eyFLP* system should be readily applicable to genetic screens addressing virtually any aspect of eye development or function. In some cases, it might prove necessary to eliminate or at least exclude from analysis the few remaining heterozygous cells. Recently, Stowers and Schwarz (1999) have presented a method similar to ours and cleverly used a *GMR-hid* transgene to kill these cells. Where these cells need not be eliminated, but merely excluded from analysis, Lee and Luo (1999) have developed an elegant method, the MARCM system, to positively rather than negatively label mutant cells. Both approaches offer potential improvements to the *eyFLP* system that may prove useful under certain conditions. For the genetic screen and phenotypic analysis we have performed using this system, however, it is of little concern that a few of the axons visualized are actually only heterozygous.

The role of PTP69D in photoreceptor axon targeting: instructive or permissive?

Garrity et al. (1999) have previously reported a low frequency of R1-R6 targeting errors in homozygous *Ptp69D* mutant larvae. These authors could not, however, examine R7 axon projections, as these are mostly established after the lethal phase of homozygous *Ptp69D* mutants. The incomplete penetrance of targeting defects of both R1-R6 and R7 axons also makes them difficult to analyse in small random clones of homozygous *Ptp69D* tissue in the adult eye. By overcoming both of these difficulties, the *eyFLP* system has allowed us to examine both R1-R6 and R7 targeting defects in *Ptp69D* mosaic adults. We have shown that PTP69D is not only required for the correct targeting of R1-R6 axons to the lamina, but also for the correct targeting of R7 axons to the medulla.

Does PTP69D play an instructive or a permissive role in photoreceptor axon targeting? In an instructive model, PTP69D might mediate signals that directly target individual axons to specific layers in the optic lobes. In a permissive model, PTP69D activation might instead promote independent pathfinding by photoreceptor growth cones, rather than continued extension along the pioneer R8 axon. In such a permissive model for PTP69D function, other signals would provide specific targeting instructions.

Although they considered both instructive and permissive models, their analysis of R1-R6 targeting errors lead Garrity et al. (1999) to favour an instructive role for PTP69D in targeting these axons to the lamina, presumably by recognizing a specific 'stop' signal in this tissue. How might an instructive model for PTP69D function explain the behaviour of R7 axons? These axons also require PTP69D for correct targeting, but appear insensitive to any 'stop' signal it might transduce in the lamina and instead interpret PTP69D activation as a 'continue' signal in the superficial layers of the medulla. Such a context-dependent interpretation of a single guidance cue is not without precedent. In tissue culture assays, the response of *Xenopus* spinal cord growth cones to gradients of the guidance cue Netrin-1 is mediated by the receptor DCC. Depending on the coexpression of another Netrin-1 receptor, UNC5 (Hong et al., 1999), or intracellular cAMP levels (Ming et al., 1997), these growth cones may be either attracted or repelled by the Netrin-1 source. In an instructive model for PTP69D function, a similar mechanism might be invoked to account for the

different responses of R1-R6 and R7 growth cones to signals transduced by PTP69D.

The permissive model, however, offers a simpler explanation for the targeting errors made by both R1-R6 and R7 axons in *Ptp69D* mutants. A common feature of many mistargeted R1-R6 axons, and probably all mistargeted R7 axons, is that they terminate in the medulla at the same level as the R8 axons. The R8 growth cone pioneers the pathway into the optic lobe. It is not known whether the R8 axon is an essential pioneer for this pathway, or whether the R1-R6 and R7 axons can independently navigate towards the optic lobe. The eight photoreceptor axons are however tightly fasciculated as they traverse the optic stalk and penetrate the brain, and it is likely that specific targeting cues for R1-R6 and R7 growth cones must counteract their adhesion to the R8 axon. PTP69D activation may reduce adhesion between photoreceptor axons, thus facilitating but not directly mediating their independent targeting decisions. In this model, the low penetrance of targeting errors in *Ptp69D* mosaics need not reflect genetic redundancy in the targeting signals, as required in the instructive model. The low penetrance may instead reflect a delicate balance between adhesive and targeting forces that is often decided in favour of targeting even without a reduction in adhesion. In our mosaic screen for visual system connectivity mutants, we recovered mutations in at least three distinct complementation groups that lead to a fully penetrant R1-R6 'passthrough' phenotype (T. P. N., B. Å., K.-A. Senti, B. J. D., unpublished). These mutations suggest that specific non-redundant targeting mechanisms may indeed exist, at least for R1-R6 axons.

Approximately half of the mistargeted R1-R6 axons in *Ptp69D* mosaics do however ultimately extend beyond the R8 terminus. A similar percentage of R7 axons also extend (correctly) beyond this layer. Perhaps the mistargeted R1-R6 axons initially stall at the level of the R8 axon terminus, but fail to find their appropriate synaptic partners in this layer. For about half of these axons, fasciculation with the R7 axon may then provide the opportunity to explore deeper regions of the medulla. Similarly, wild-type R1-R6 axons that have initially targeted the lamina will resume growth along R7 and R8 axons into the medulla if their final choice of targets is blocked pharmacologically (Gibbs and Truman, 1998).

PTP69D is also required for correct targeting of motor axons in the embryo, and here too it has been assigned a permissive role in axon guidance (Desai et al., 1996, 1997). Motor axons lacking PTP69D and other RPTPs also fail to exit common nerve pathways, leading to characteristic 'bypass' and 'stall' phenotypes that are highly reminiscent of the behaviour of mutant R1-R6 and R7 axons respectively in the visual system. In the embryo, these defects are mimicked by increasing the levels of the homophilic cell adhesion molecule FasciclinII (Lin and Goodman, 1994), leading to the suggestion that PTP69D activation at specific choice points might help counter FasciclinII-mediated adhesion (Desai et al., 1996). Photoreceptor axons also express FasciclinII, as well as several other cell adhesion molecules of the immunoglobulin, leucine-rich repeat, and cadherin families (Krantz and Zipursky, 1990; Ramos et al., 1993; T. P. N., K-A. Senti, and B. J. D., unpublished). Altering the levels of these molecules, in both wild-type and *Ptp69D* mutant backgrounds, should help define the molecular pathways by which PTP69D reduces adhesion between photoreceptor axons to facilitate the transition from fasciculative to independent navigation.

We thank Ernst Hafen and Corey Goodman for their generous support during the initial stages of this work, Eva Niederer, Dina El Tounsy and Rita Bopp for excellent and tireless technical assistance during the connectivity screen, Wen-Hai Chou and Steve Britt for advice on the immunofluorescent staining of adult head sections, Peder Zipperlin for sequence analysis, and Karin Paiha and Peter Steinlein for assistance with confocal microscopy and image processing. We also thank Kathy Matthews and the Bloomington Drosophila Stock Center for providing and accepting *Drosophila* stocks, Larry Zipursky for generously providing mAb24B10, fly stocks, and valuable technical and scientific advice, Kai Zinn, Uwe Walldorf, John Thomas, Gerry Rubin, Konrad Basler, Steve Cohen and Brian Mozer for various reagents, and Jürgen Knoblich and Annette Neubüser for suggestions to improve the manuscript. We are particularly indebted to Uwe Walldorf for providing details on the *eyeless* enhancer prior to publication. During the initial development of the *eyFLP* system, B. J. D. was a postdoctoral fellow in the laboratory of Corey Goodman, supported by a fellowship from the Helen Hay Whitney Foundation. B. Å. was supported by a postdoctoral fellowship from the Wenner-Gren Foundation. Much of this work was conducted at the University of Zurich with the support of the Swiss National Science Foundation.

REFERENCES

Boschert, U., Ramos, R. G., Tix, S., Technau, G. M. and Fischbach, K. F. (1990). Genetic and developmental analysis of *irreC*, a genetic function required for optic chiasm formation in Drosophila. *J. Neurogenet.* **6**, 153-171.

Callahan, C. A. and Thomas, J. B. (1994). Tau-beta-galactosidase, an axon-targeted fusion protein. *Proc. Natl. Acad. Sci. USA* **91**, 5972-5976.

Chou, W. H., Huber, A., Bentrop, J., Schulz, S., Schwab, K., Chadwell, L. V., Paulsen, R. and Britt, S. G. (1999). Patterning of the R7 and R8 photoreceptor cells of *Drosophila*: evidence for induced and default cell-fate specification. *Development* **126**, 607-616.

Desai, C. J., Gindhart, J. G., Jr., Goldstein, L. S. and Zinn, K. (1996). Receptor tyrosine phosphatases are required for motor axon guidance in the Drosophila embryo. *Cell* **84**, 599-609.

Desai, C. J., Krueger, N. X., Saito, H. and Zinn, K. (1997). Competition and cooperation among receptor tyrosine phosphatases control motoneuron growth cone guidance in *Drosophila*. *Development* **124**, 1941-1952.

Fortini, M. E. and Rubin, G. M. (1990). Analysis of cis-acting requirements of the *Rh3* and *Rh4* genes reveals a bipartite organization to rhodopsin promoters in Drosophila melanogaster. *Genes Dev.* **4**, 444-463.

Freeman, M. (1997). Cell determination strategies in the *Drosophila* eye. *Development* **124**, 261-270.

Fujita, S. C., Zipursky, S. L., Benzer, S., Ferrus, A. and Shotwell, S. L. (1982). Monoclonal antibodies against the Drosophila nervous system. *Proc. Natl. Acad. Sci. USA* **79**, 7929-7933.

Garrity, P. A., Rao, Y., Salecker, I., McGlade, J., Pawson, T. and Zipursky, S. L. (1996). Drosophila photoreceptor axon guidance and targeting requires the dreadlocks SH2/SH3 adapter protein. *Cell* **85**, 639-650.

Garrity, P. A., Lee, C. H., Salecker, I., Robertson, H. C., Desai, C. J., Zinn, K. and Zipursky, S. L. (1999). Retinal axon target selection in Drosophila is regulated by a receptor protein tyrosine phosphatase. *Neuron* **22**, 707-717.

Gibbs, S. M. and Truman, J. W. (1998). Nitric oxide and cyclic GMP regulate retinal patterning in the optic lobe of Drosophila. *Neuron* **20**, 83-93.

Golic, K. G. (1991). Site-specific recombination between homologous chromosomes in Drosophila. *Science* **252**, 958-961.

Goodman, C. S. (1996). Mechanisms and molecules that control growth cone guidance. *Ann. Rev. Neurosci.* **19**, 341-77

Hauck, B., Gehring, W. J. and Walldorf, U. (1999). Functional analysis of an eye specific enhancer of the *eyeless* gene in Drosophila. *Proc. Natl. Acad. Sci. USA* **96**, 564-569.

Hay, B. A., Wolff, T. and Rubin, G. M. (1994). Expression of baculovirus P35 prevents cell death in *Drosophila*. *Development* **120**, 2121-2129.

Hing, H., Xiao, J., Harden, N., Lim, L. and Zipursky, S. L. (1999). Pak functions downstream of Dock to regulate photoreceptor axon guidance in Drosophila. *Cell* **97**, 853-863.

Hong, K., Hinck, L., Nishiyama, M., Poo, M. M., Tessier-Lavigne, M. and Stein, E. (1999). A ligand-gated association between cytoplasmic domains of UNC5 and DCC family receptors converts netrin-induced growth cone attraction to repulsion. *Cell* **97**, 927-941.

Hummel, T., Schimmelpfeng, K. and Klambt, C. (1999). Commissure formation in the embryonic CNS of Drosophila: I. Identification of the required gene functions. *Dev Biol* **209**, 381-398.

Kolodziej, P. A., Jan, L. Y. and Jan, Y. N. (1995). Mutations that affect the length, fasciculation, or ventral orientation of specific sensory axons in the Drosophila embryo. *Neuron* **15**, 273-286.

Krantz, D. E. and Zipursky, S. L. (1990). Drosophila chaoptin, a member of the leucine-rich repeat family, is a photoreceptor cell-specific adhesion molecule. *EMBO J.* **9**, 1969-1977.

Kunes, S. (1999). Stop or go in the target zone. *Neuron* **22**, 639-640.

Kunes, S., Wilson, C. and Steller, H. (1993). Independent guidance of retinal axons in the developing visual system of Drosophila. *J. Neurosci.* **13**, 752-767.

Lee, T. and Luo, L. (1999). Mosaic analysis with a repressible cell marker for studies of gene function in neuronal morphogenesis. *Neuron* **22**, 451-461.

Lin, D. M. and Goodman, C. S. (1994). Ectopic and increased expression of Fasciclin II alters motoneuron growth cone guidance. *Neuron* **13**, 507-523.

Martin, K. A., Poeck, B., Roth, H., Ebens, A. J., Ballard, L. C. and Zipursky, S. L. (1995). Mutations disrupting neuronal connectivity in the Drosophila visual system. *Neuron* **14**, 229-240.

Meinertzhagen, I. and Hanson, T. E. (1993). The development of the optic lobe. In *The Development of Drosophila melanogaster* (ed. A. Martinez Arias and M. Bate), pp. 1363-1490. New York: Cold Spring Harbor Press.

Ming, G. L., Song, H. J., Berninger, B., Holt, C. E., Tessier-Lavigne, M. and Poo, M. M. (1997). cAMP-dependent growth cone guidance by netrin-1. *Neuron* **19**, 1225-1235.

Mismer, D. and Rubin, G. M. (1987). Analysis of the promoter of the *ninaE* opsin gene in Drosophila melanogaster. *Genetics* **116**, 565-578.

Morata, G. and Ripoll, P. (1975). Minutes: mutants of Drosophila autonomously affecting cell division rate. *Dev. Biol.* **42**, 211-221.

Moses, K. and Rubin, G. M. (1991). Glass encodes a site-specific DNA-binding protein that is regulated in response to positional signals in the developing Drosophila eye. *Genes Dev.* **5**, 583-593.

Mozer, B. A. and Benzer, S. (1994). Ingrowth by photoreceptor axons induces transcription of a retrotransposon in the developing *Drosophila* brain. *Development* **120**, 1049-1058.

Ramos, R. G., Igloi, G. L., Lichte, B., Baumann, U., Maier, D., Schneider, T., Brandstatter, J. H., Frohlich, A. and Fischbach, K. F. (1993). The *irregular chiasm C-roughest* locus of Drosophila, which affects axonal projections and programmed cell death, encodes a novel immunoglobulin-like protein. *Genes Dev.* **7**, 2533-2547.

Seeger, M., Tear, G., Ferres-Marco, D. and Goodman, C. S. (1993). Mutations affecting growth cone guidance in Drosophila: genes necessary for guidance toward or away from the midline. *Neuron* **10**, 409-426.

Stowers, R. S. and Schwarz, T. L. (1999). A genetic method for generating Drosophila eyes composed exclusively of mitotic clones of a single genotype. *Genetics* **152**, 1631-1639.

Streuli, M., Krueger, N. X., Thai, T., Tang, M. and Saito, H. (1990). Distinct functional roles of the two intracellular phosphatase like domains of the receptor-linked protein tyrosine phosphatases LCA and LAR. *EMBO J.* **9**, 2399-2407.

Tear, G. (1999). Neuronal guidance. A genetic perspective. *Trends Genet.* **15**, 113-118.

Tessier-Lavigne, M. and Goodman, C. S. (1996). The molecular biology of axon guidance. *Science* **274**, 1123-1133.

Thomas, B. J. and Wassarman, D. A. (1999). A fly's eye view of biology. *Trends Genet.* **15**, 184-190.

Tomlinson, A. and Ready, D. F. (1987). Neuronal differentiation in the Drosophila ommatidium. *Dev. Biol.* **120**, 366-376.

Weiss, A. and Schlessinger, J. (1998). Switching signals on or off by receptor dimerization. *Cell* **94**, 277-280.

Wills, Z., Bateman, J., Korey, C. A., Comer, A. and Van Vactor, D. (1999). The tyrosine kinase Abl and its substrate enabled collaborate with the receptor phosphatase Dlar to control motor axon guidance. *Neuron* **22**, 301-312.

Wolff, T., Martin, K. A., Rubin, G. M. and Zipursky, S. L. (1997). The Development of the *Drosophila* Visual System. In *Molecular and Cellular Approaches to Neural Development* (ed. W. M. Cowan, T. M. Jessell and S. L. Zipursky), pp. 474-508. Oxford: Oxford University Press.

Xu, T. and Rubin, G. M. (1993). Analysis of genetic mosaics in developing and adult *Drosophila* tissues. *Development* **117**, 1223-1237.